MULTI-POINT AERODYNAMIC OPTIMIZATION BY MEANS OF MEMETIC ALGORITHM FOR DESIGN OF ADVANCED TILTROTOR BLADES

Andrea Massaro
andrea.massaro@agustawestland.com
Rotor Aerodynamics Specialist
AgustaWestland, Aerodynamics Dept.
Italy

Andrea D'Andrea
andrea.dandrea@agustawestland.com
Rotor Aerodynamics Technical Leader
AgustaWestland, Aerodynamics Dept.
United Kingdom

Abstract

A multi-objective and multi-point optimization framework for tiltrotor blade performance enhancement is presented. This framework is based on a multi-objective surrogate-assisted memetic algorithm which is coupled with different aerodynamic solvers and can improve separately airfoils and rotor planform/twist distributions. The purpose is to improve aerodynamic performance of tiltrotor rotors in multi-point flight operations by searching for optimal blade shape with excellent behavior for both hover and propeller. The optimization procedure and the memetic algorithm are first described. Afterwards, they are applied to the improvement of the XV15 rotor airfoils and blade. The outcomes from the related optimizations are presented and discussed from an aerodynamic viewpoint. The advantages of the proposed procedure for aerodynamic optimization of tiltrotor blades are finally highlighted.

1 INTRODUCTION

The tiltrotors technology have been extensively studied and developed in the last decades thanks to the interest that such a concept inspired and the advantages over traditional aircrafts. Tiltrotors combine the peculiar vertical takeoff capability of a helicopter with the cruise speed of a proprotor. Since the extremely different airflow conditions that a tiltrotor rotor sees converting from hover to cruise, the rotor aerodynamic design is a crucial aspect in order to obtain an efficient and effective tiltrotor global design.

The early stage of the tiltrotor development started with the XV-3 concept of convertible aircraft already in the '50s thanks to the cooperation of NASA and Bell which encountered initial technical issues mainly due to whirl-flutter instabilities. The first tiltrotor designs were followed by the XV15[1] aircraft in the '70s and '80s. The research aircraft XV3 and XV15 made a major contribution to the development of the Bell-Boeing V-22 Osprey now on service and the AW609 tiltrotor now held by AgustaWestland. More recent concepts have been studied like the ERICA tiltrotor within the European Community. The rotor aerodynamics design for tiltrotors followed a similar path with consequent improvements during the years up to the current technologies installed on the V-22 and AW609 aircrafts. The numerical capabilities that are nowadays available in computational fluid dynamics in terms of performance prediction accuracy and the related computational capabilities enabled by HPCs (High Performance Computers) allow the further improvements of tiltrotor rotor performance, highly reducing the compromises between hover and propeller rotor efficiencies.

The paper presents the work done by AgustaWestland on the development of an integrated and efficient framework for the numerical aerodynamics optimization of airfoils and rotor blades for tiltrotor applications, together with preliminary optimization outcomes which represent the base for future further improvements.

2 OPTIMIZATION FRAMEWORK

The optimization framework is composed of several tools. First a multi-objective Surrogate-Assisted Memetic Algorithm (SAMA) is developed and presented which manages the codes to solve airfoil/rotor aerodynamic solutions. Second, the aforementioned codes are described.

2.1 Multi-Objective Optimizer (Surrogate-Assisted Memetic Algorithm)

The core of the optimization framework is a state-of-the-art Multi-Objective evolutionary algorithm which is able to solve Multi-Objective and Multi-Point problems using a very efficient strategy of optimization. The strategy is based on a two-level optimization process and the use of surrogate models to speed up the optimization and reduce the overall time by diminishing the number of aerodynamic simulations required. The algorithm is also known as Surrogate-Assisted Memetic Algorithm (SAMA) and uses a first-level optimization algorithm, which is a common Genetic Algorithm (GA), and a second-level optimization algorithm, which is a gradient-based SQP. This second-level algorithm is used together with a mathematical approximation of the aerodynamic performance of the airfoil/rotor to be optimized (this mathematical approximation is also called Surrogate model) which is much faster than the aerodynamic airfoil/rotor

solver during the evaluation phase (few seconds versus hours needed, for example, for a hover computation) and contemporary ensure very low approximation errors if compared to the aerodynamic solution. The Surrogate model needs an initial database of aerodynamic solutions which are periodically updated and enlarged during the optimization course of events, increasing also the accuracy of the approximated model. A schematic representation of the SAMA optimizer's course of events is depicted in Figure 1.

Such a methodology permits limited time and hardware infrastructures for airfoil and rotor optimizations thanks to its efficiency, in addition it easily manages real engineering problems being intrinsically Multi-Objective. The methodology has been extensively used and validated for previous optimization works of airfoils[2], helicopter rotors[3] and low noise helicopter landing trajectories[4]. For the present work it requires several aerodynamic tools to be coupled in order to be able to optimize the aerodynamic shape of airfoils and blades for tiltrotor applications. Follows a description of the main tools coupled.

2.2 Airfoil 2D Solver

The CFD solver Fluent has been coupled to the above optimizer in order to allow the framework to generate optimal 2D airfoils specifically developed for the use on tiltrotor blades. The fact that on a tiltrotor the rotors must work efficiently in hover as well as in propeller mode makes the optimization of such airfoils highly challenging due to the variability of the operative conditions, leading to optimizations with many conditions (Multi-Point optimizations) to be taken into account with several objectives (high maximum lift for hover and high drag divergence Mach for propeller) and constraints (low pitching moments and geometric constraints).

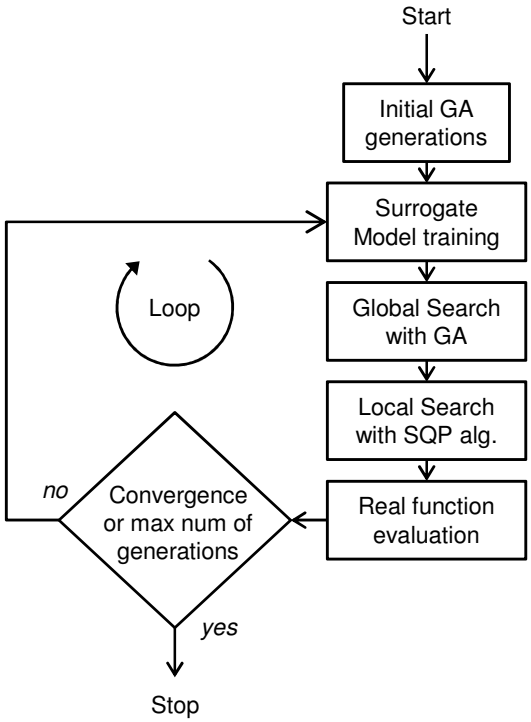

Figure 1: Optimizer workflow.

The implemented 2D airfoil's numerical model is based on a O-shape fully structured mesh with approximately 75k cells and 500 points on the airfoil's surface. The flowfield is considered as fully-turbulent (no laminar-turbulent transition is simulated) and the boundary layer velocity field is completely resolved (a refined mesh at the wall with $y^+ \approx 1$ is used). The turbulence model utilized is the 1eq Spalart-Allmaras.

The optimization framework is capable of managing the entire process to aerodynamically simulate the airfoil shapes that the optimizer itself produces during the ongoing optimization. The process requires a preliminary mesh generation and then the Fluent simulations run in parallel for several airfoils (the SAMA method is a population-based algorithm) and several flow conditions, collecting the results and converting them into the optimization objectives.

2.3 Rotor Simulation Tools

A 3D panel method is coupled to the optimizer for the accurate simulation of rotors in hover and propeller mode. The panel method is here selected since its efficiency and accuracy when compared to other methods. In particular the aerodynamic solver is the AgustaWestland in-house solver ADPANEL[5], which is a Full-Unstructured Multi-Processor Panel code coupled with a Time-Stepping Non-Linear Free Wake Vortex model. This tool implements the most advanced aerodynamic features in the field of potential methods, in particular for the Constant Vorticity Contour (CVC) modeling of both rotary and fixed wing wakes. Thanks to the previous features, ADPANEL is able to analyze in short computational times and with detailed predictions entire helicopter and tiltrotor configurations even operating in ground effect. The wake modeling implemented in ADPANEL is composed of two parts: a "dipole buffer wake sheet", and a set of "constant vorticity contour vortex filaments". Buffer wake and CVC vortex filaments are used to represents the vorticity released from rotary and fixed wings for both their components, trailed and shed. The CVC free-wake modeling developed in ADPANEL allows to generate refined roll-ups and high spanwise resolution along rotor blades without enforcing an unnecessary large number of wake elements. Figure 2 shows an example of the computed CVC wake development in case of a full-helicopter configuration operating in OGE (left) and the wake developed by the ERICA tiltrotor in conversion mode (right).

The ADPANEL code requires much less computational resources than a traditional CFD

method with sufficient accuracy in terms of performance prediction for the more common helicopter/tiltrotor flight conditions, thus highly limiting the total computational effort. Even if the ADPANEL accuracy has been extensively proven for both helicopter and tiltrotor rotors, the Navier-Stokes (N-S) fully-structured solver HMB[6] is used to validate the optimal results obtained with the panel method. It must be noted that the HMB solver uses here the SST k-ω turbulence model and the flow is considered fully turbulent (no transitional modeling is used) and no corrections are applied to the viscous torque to take into account the possible reduction due to laminarity of the boundary layer.
ADPANEL does not trim the rotor for required thrust level, therefore the Camrad/JA[7] tool is used together with ADPANEL to provide a good guess value for the collective pitch. This does not assure a correct trim of the rotor within ADPANEL, so the collective pitch value (for each simulated condition) is considered as a free variable for the optimizer that, contemporarily with the main optimization problem, tends to converge to the correct collective for the required amount of thrust. Once again, the optimization framework is able to manage the aforementioned tools (Camrad/JA with ADPANEL) in order to get the performance prediction of several rotor blades in different flight conditions.

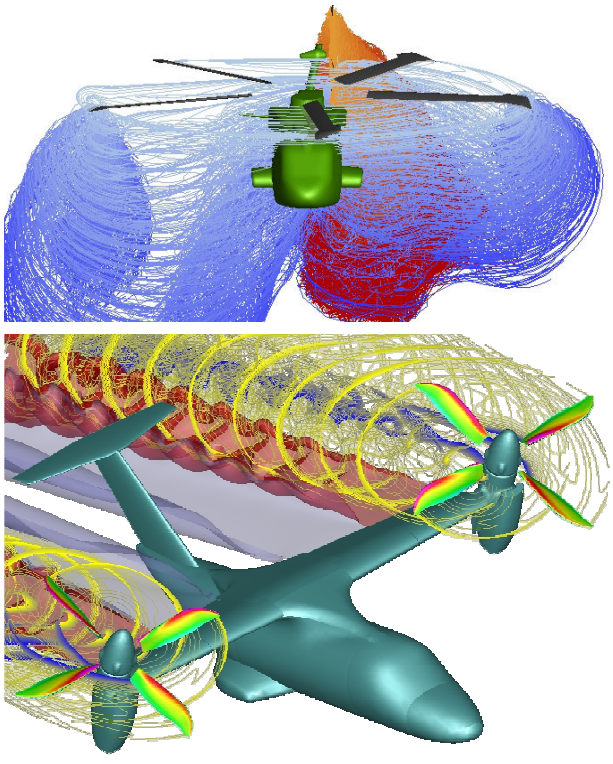

Figure 2: ADPANEL CVC wake development for a full-helicopter configuration (top) and a tiltrotor configuration (bottom).

3 OBJECTIVES OF THE PAPER

In the present work the developed optimization framework has been applied to a case study to prove its capabilities in optimizing rotor blades and airfoils for tiltrotor applications. The selected baseline rotor is the one installed on the XV15 tiltrotor. It is available in open literature in terms of airfoils (coming from the NACA 64-series) and blade planform/twist[8]. The optimization activities are subdivided into two main steps as follows:

3.1 Rotor Airfoil Optimizations

The four generative airfoils used on the XV15 blade[8] (respectively of 28%, 18%, 12% and 8% thickness) have been optimized taking into account the typical operative conditions of the aircraft (both hover and propeller). For these reasons a wide and deep preliminary study of the baseline rotor has been conducted in order to define the correct operative conditions for each generative airfoil.
Table 1 describes the outcomes of the XV15 rotor study with the main driven objectives used to determine each optimization problem.
As an example, the translation of the driven objectives into mathematical objectives is reported for the 8% thickness airfoil (used at the blade tip). The optimization is Multi-Point, it takes into account the different operative conditions (as visible in Table 2), and Multi-Objective, since the two different objectives in Eq. 1. The nature of the objectives is clear, the first one Obj_1 is defined in order to maximize the $C_{l,max}$ at several Mach numbers, which is worth for maximum thrust capabilities and maneuverability. The Obj_2 is defined in order to minimize the drag in propeller (high Mach and very low angles) and extend as much as possible the drag divergence Mach. In addition to this, several constraints are set to guarantee the 8% thickness, the pitching moment limitation and the superiority at all the conditions respect to the baseline airfoil.
Similar problems are set for the remaining thicker airfoils.

Airfoil t/c%	Radial station [r/R]	Main driven objectives	
		Hover and Maneuver	Propeller
		Maxim. of lift, Mach range	Minim. of drag, Mach range
28%	0.2	0.2-0.3 @ SL	0.4-0.5 @ 20000ft, C_l=0
18%	0.5	0.3-0.4 @ SL	0.45-0.6 @ 20000ft, C_l=0
12%	0.8	0.4-0.65 @ SL	0.55-0.75 @ 20000ft, C_l=0.2
8%	1.0	0.45-0.75 @ SL	0.7-0.85 @ 20000ft, C_l=0.2

Table 1: Main driven objectives of the optimization process for the four XV15 airfoils.

Cond	Mach	Re[x10^6]	AoA[deg]	Ambient
C1	0.45	3.72	11	ISA SL
C2	0.55	4.56	8	ISA SL
C3	0.65	5.38	6	ISA SL
C4	0.75	6.21	5	ISA SL
C5	0.7	3.22	0	ISA 20000ft
C6	0.75	3.46	-0.1	ISA 20000ft
C7	0.85	3.92	-0.5	ISA 20000ft

Table 2: Operative conditions selected for the 8% thickness airfoil optimization.

$$(1)\quad \begin{cases} \mathrm{Obj}_1 = \max(C_{l,C3} + C_{l,C4}) \\ \mathrm{Obj}_2 = \min(2C_{d,C5} + 2C_{d,C6} + C_{d,C7}) \end{cases}$$

$$(2)\quad \begin{cases} t/c \geq 8\% \\ C_{l,C1} \geq C_{l,C1,XV-15} \\ C_{l,C2} \geq C_{l,C2,XV-15} \\ C_{l,C3} \geq C_{l,C3,XV-15} \\ C_{l,C4} \geq C_{l,C4,XV-15} \\ C_{l,C5} \geq C_{l,C5,XV-15} \\ C_{d,C5} \leq C_{d,C5,XV-15} \\ C_{d,C6} \leq C_{d,C6,XV-15} \\ \left|C_{m1/4,C5}\right| \leq \left|C_{m1/4,C5,XV-15}\right| \end{cases}$$

3.2 Rotor Blade Optimization

After the airfoil optimizations the entire blade is considered for the aerodynamic optimization aimed at the performance improvement of the rotor. Several blade features have been considered during the optimization, which are:

- **Twist:** with 7 control variables;
- **Chord:** with 3 control variables. One is used to control the rotor solidity as a coefficient that multiplies the chord distribution in the range ±15%. The other two are used to control the tip geometry, allowing a parabolic-like smooth change in tip chord starting from the 75% of the rotor radius;
- **Sweep:** with 2 control points (localized at the tip region). The two points are used to allow the optimizer to move the quarter chord locus on the rotor plane starting from the 75% of the rotor radius;
- **Anhedral:** with 1 control point (localized at the tip region) starting from 90% of the rotor radius.

As an example the parameterization method used for the twist is shown in Figure 3. The baseline twist of the XV-15 is reproduced by means of a b-spline. The control points of the b-spline are free variables for the optimizer.

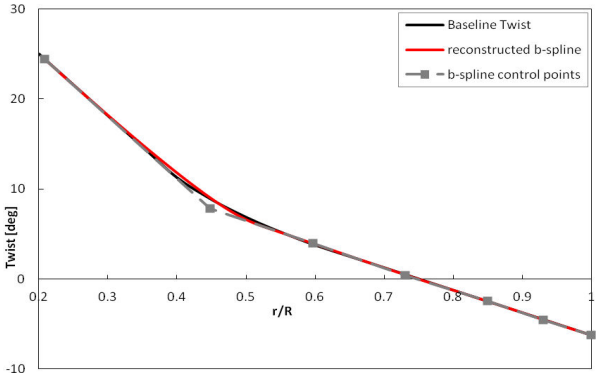

Figure 3: Parameterization method for the blade twist.

The rotor blade optimization has the following two objectives (solved simultaneously thanks to the multi-objective approach of the implemented optimizer):

Obj 1: Maximization of the FoM in Hover condition for a C_t = 0.012.
Obj 2: Maximization of the Propulsive Efficiency in Propeller condition for a range of C_t going from 0.002 to 0.006. The flight condition selected is ISA+0° at 20000ft altitude with a TAS of 280 kts

The constraints of the problem are:

Constr 1: The FoM in Hover condition for a C_t = 0.008 must be higher than or equal to the one of the XV15 rotor.
Constr 2: The FoM in Hover condition for a C_t = 0.014 must be higher than or equal to the one of the XV15 rotor.

During the optimization the rotor radius is kept constant (equal to 3.81 m) and the tip speed for hover and propeller conditions are fixed to 235.1 m/s and 204.1 m/s respectively, corresponding to tip Mach numbers of 0.691 and 0.6 (calculated at ISA+0° Sea Level).

4 BASELINE ROTOR PERFORMANCE

The XV15 rotor is here selected as reference technology for the performance optimization. The rotor is simulated with the numerical tools ADPANEL and HMB involved in the optimization and validation process respectively, in order to compare them against the available experimental data. The validation of the tools is performed in Hover[9],[10],[11] and Propeller[12] conditions. The latter consists in a air speed of 185 kts (approximately Sea Level ambient conditions) and a tip Mach number of 0.54. Following figures represent the numerical models used with ADPANEL (Figure 4) and HMB (Figure 5). Figure 6 and Figure 7 show the outcomes of the validation phase. Both the codes used here correlate in a very excellent way the experimental data,

especially the Hover ones. The Propeller case shows very good agreement for the lowest C_t available, while seems to slightly underestimate

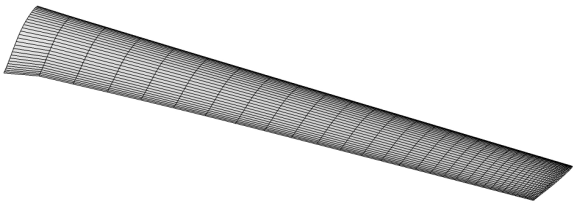

Figure 4: ADPANEL surface mesh for the XV15 blade.

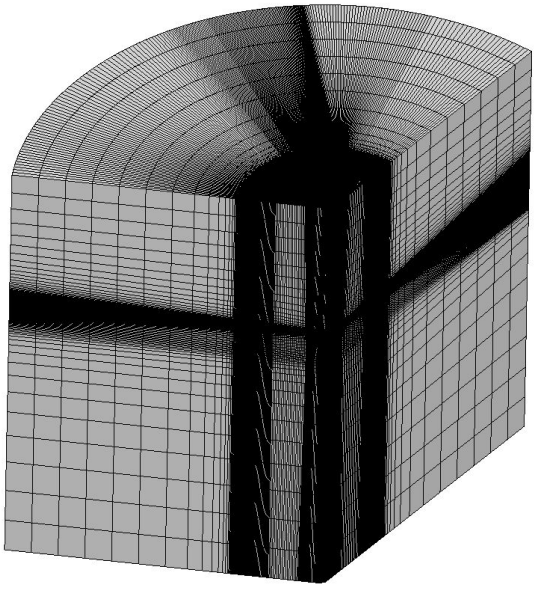

Figure 5: HMB volume mesh (periodic) for the XV15 blade for Hover calculation.

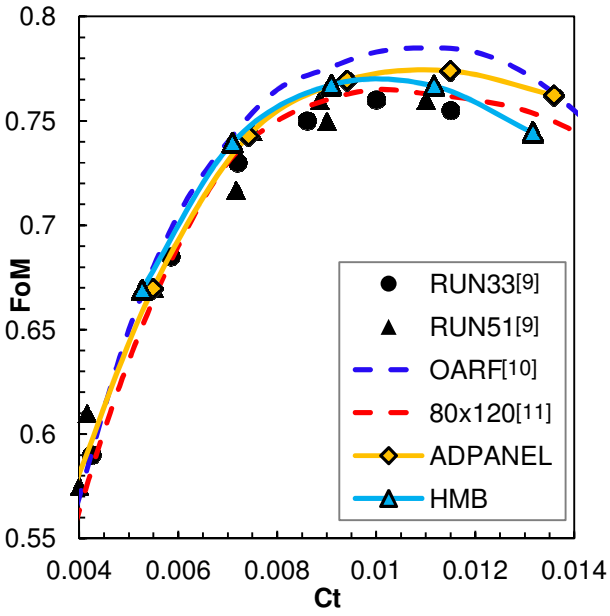

Figure 6: Figure of Merit of the Baseline XV15 rotor. Numerical predictions with ADPANEL and HMB compared to experimental data[9],[10],[11].

efficiency for the highest C_t. It is worth noting that the two codes present very similar behavior for all the conditions tested in the validation phase, a

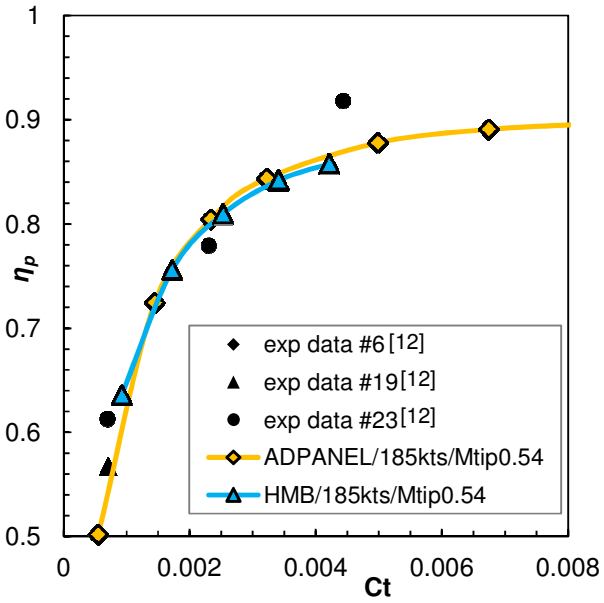

Figure 7: Propeller Efficiency of the Baseline XV15 rotor. Numerical predictions with ADPANEL and HMB compared to experimental data[12].

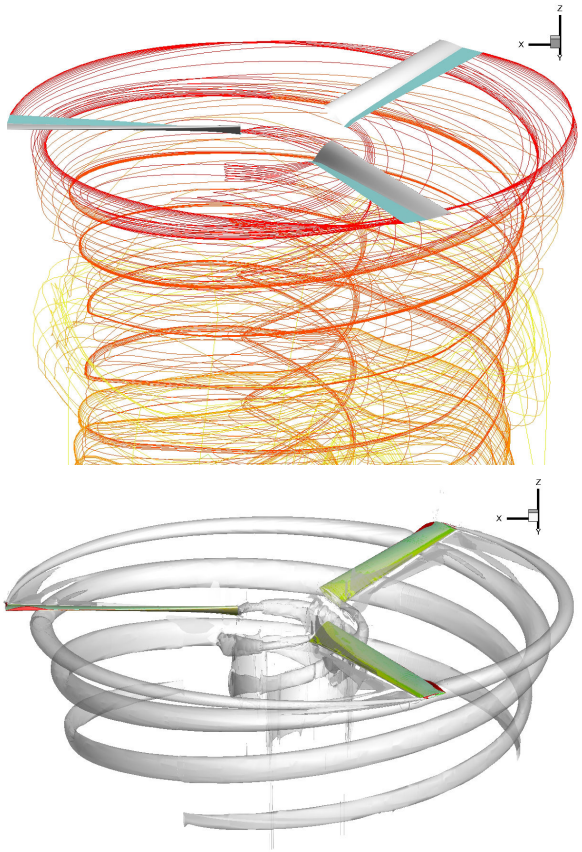

Figure 8: Comparison of the ADPANEL (top) and HMB (bottom) model behavior for a Hover case ($C_t \approx$ 0.011) of the XV15 rotor.

part some small discrepancies when the rotor is close to the stall in Hover.

5 RESULTS

The present section contains the outcomes of the optimization of airfoils and rotor blade. Regarding the airfoils the new geometries are presented and compared to the original XV15 airfoils. The rotor has been tested with the new airfoils in order to quantify the benefits in terms of global performance. Second the planform/twist optimization of the rotor blade is shown with the related results.

5.1 Results of the Rotor Airfoil Optimizations

The results of the four airfoil optimizations performed (and described in § 3.1) are presented in Figure 9. Each optimal airfoil comes from a multi-objective/multi-point optimization process and is one of a set of optimal solutions (the Pareto front, not reported here for brevity). Therefore the final optimal solution is selected among the aforementioned Pareto front by the user in order to obtain the best compromise in terms of performance improvement. The four optimal geometries are then compared with the baseline XV15 generative airfoils showing the main differences. The maximization of the $C_{l,max}$ led to more pronounced noses while maintaining or improving also the performance in transonic conditions. The limitation in pitching moment then led to a general rearrangement of the global shape (lower side near the trailing edge).
The outcomes in terms of airfoil's performance are visible in Figure 10 and Figure 11 where the $C_{l,max}$ and the M_{dd} are plotted respectively. The $C_{l,max}$ is calculated in function of the radial station (so it changes in function of the specific airfoil used along the blade) and the local Mach number as coming from a Hover flight (with M_{tip} = 0.691). It can be seen how the largest improvements are obtained for the airfoil with t/c of 18% and decrease as the thickness decreases. The 8% t/c airfoil at the tip is not improved since the small thickness which limits the achievable $C_{l,max}$. The improvements in M_{dd} is more limited (approximately 0.015) but uniformly distributed along the radial station. The local Mach number reached when in flight by the rotor is also plotted for the Hover case and for Propeller flight at 280 kts and ISA+0° 20000ft altitude. Here the helical Mach number is plotted having more significance. It is possible to note how the most critical zone is the outer part of the blade.
The new optimal airfoils have been tested on the XV15 original blade planform/twist for Hover and Propeller (Figure 12 and Figure 13 respectively). It is clear that the improvements obtained slightly impacts the global performance of the rotor with the XV15 fixed planform. In Hover the FoM is improved as the C_t approaches high values (beginning of stall) thanks to the locally increased $C_{l,max}$. On the contrary, the limited improvement of M_{dd} slightly

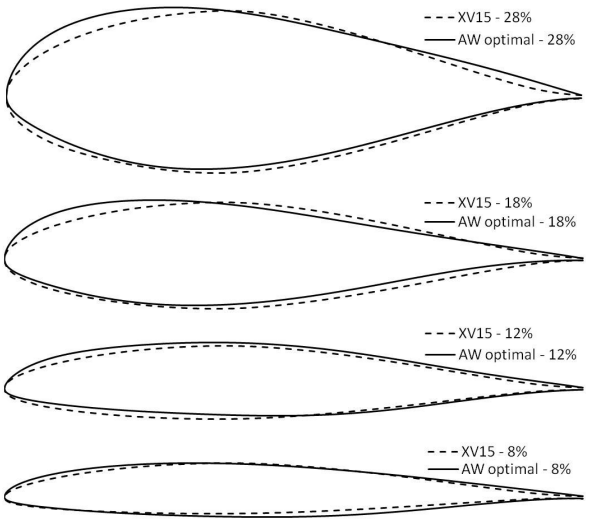

Figure 9: AW optimal airfoil geometries coming from the optimizations. Comparison with the baseline airfoils of the XV15 rotor.

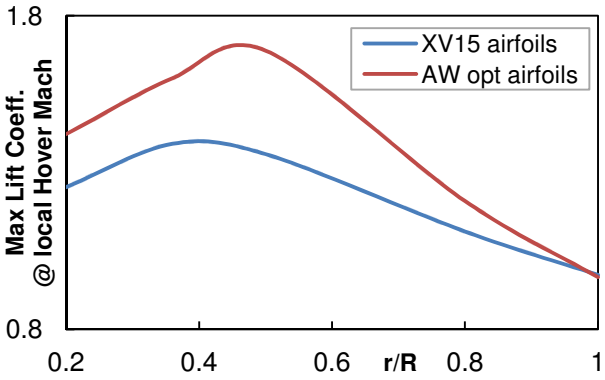

Figure 10: Maximum lift coefficient of the airfoils calculated at the local hover Mach number. Comparison between the baseline XV15 airfoils and the optimized ones.

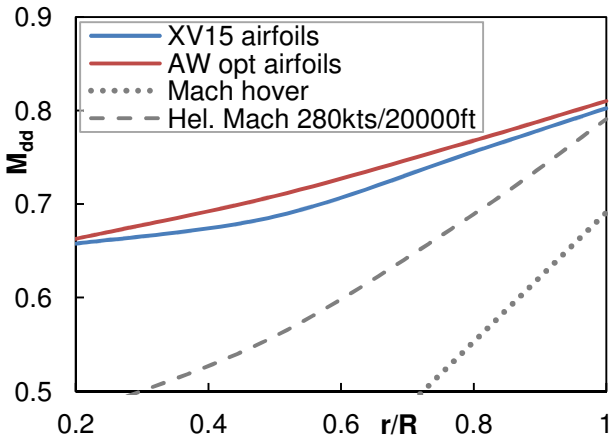

Figure 11: Drag-divergence Mach number, calculated at C_t=0. Comparison between the baseline XV15 airfoils and the optimized ones.

affects the Propeller Efficiency for the range of C_t of 0 – 0.004. This is due to the drag reduction related to the M_{dd} increase but as the thrust increases the airfoils work at C_l approaching 0.2-0.3 (or higher) reducing the M_{dd} and the delta between the two technologies (XV15 and AW optimal airfoils)

5.2 Results of the Rotor Blade Optimization

The results of the blade planform/twist optimization are here presented to demonstrate the capabilities of the optimization framework and the possible performance improvements achievable for the XV15 tiltrotor blade.

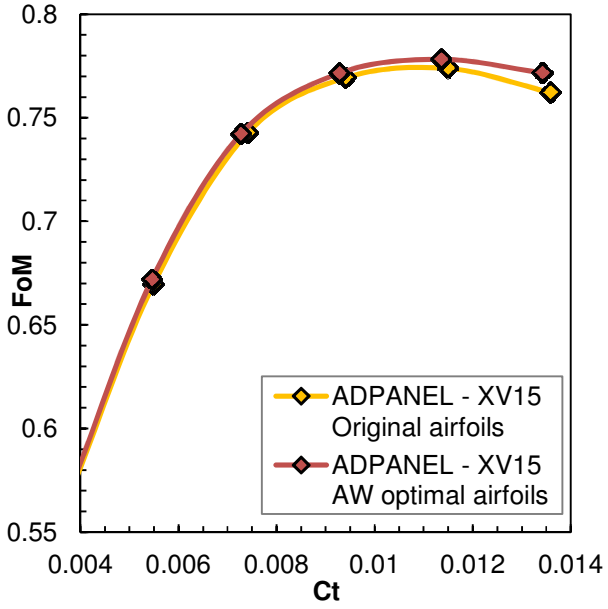

Figure 12: Figure of Merit of the XV15 rotor blade with original XV15 airfoils and new optimized airfoils (planform and twist is unchanged).

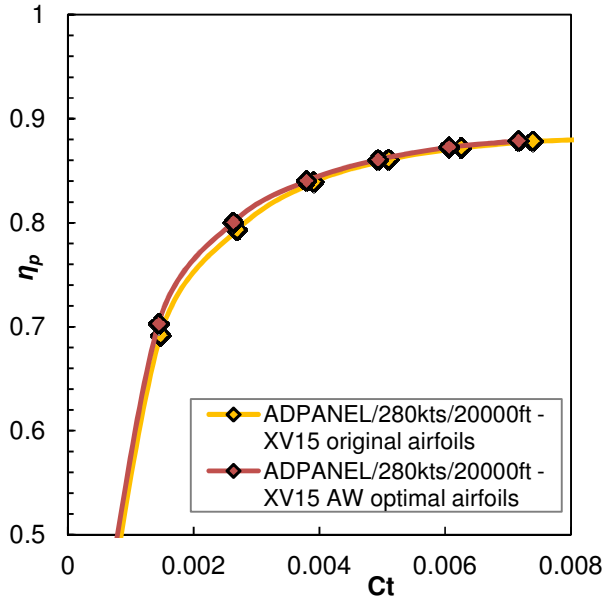

Figure 13: Propeller Efficiency of the XV15 rotor blade with original XV15 airfoils and new optimized airfoils (planform and twist is unchanged). 280 KTAS at ISA+0° 20000ft.

The optimization involves two main objectives (see § 3.2), one related to the hover FoM maximization at fixed thrust and the second the maximization of propulsive efficiency in propeller mode for a range of C_t (from 0.002 to 0.006) at 280 kts, 20000 ft altitude condition. Since the second objective is related to a range of thrust levels it is calculated integrating over the C_t the propulsive efficiency.

The resulting optimal solutions are visible in Figure 14 plotted as percentage improvements of FoM and η_P with respect to the baseline XV15 performance. The ADPANEL FoM estimation is selected as baseline for hover (abscissa), having a value of 0.773, while the integration of the propulsive efficiency over the C_t (ordinate) is not reported. Since the multi-objective nature of the problem, the optimal solutions lie on the Pareto front set (highlighted in Figure 14 with red diamonds). Three among the optimal solutions are selected for additional investigations regarding their geometric features and aerodynamic performance, selected in order to cover the Pareto front extension. They are called respectively P1 (best hover, worst prop), P3 (compromise) and P7 (worst hover, best prop).

The P1 solution is capable of FoM slightly above 0.8 (increase of 3.8% respect to the XV15 at C_t = 0.012) with a good increase in propeller anyway. The P7, instead, reaches propeller efficiency improvements of about 8% with a maximum FoM of about 0.793. The P3 solution is a compromise between the two extreme solutions having a FoM of 0.8 and a 6.4% improvement of performance in propeller. The three optimal solutions are then compared in terms of geometric features from Figure 15 to Figure 18.

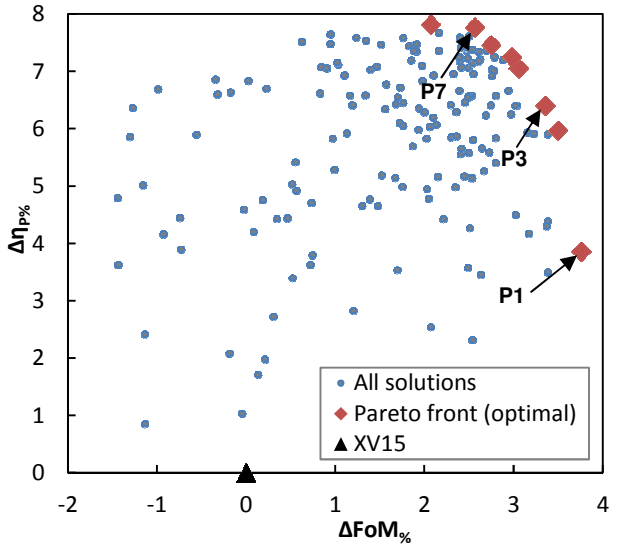

Figure 14: Percentage improvements of the resulting optimal solutions for FoM (abscissa) and η_P (ordinate). The optimal set (or Pareto front) is highlighted.

Figure 15 shows the chord distributions. The baseline XV15 rotor has a thrust weighted solidity of 0.089, while the selected optimal rotors have solidity of 0.0851, 0.0887 and 0.0843 (for P1, P3 and P7 respectively). The reduction in solidity is essentially due to the tip reduction in chord that is partially counterbalanced by an increase in the straight part of the blade. The chord reduction at the tip together with a quarter chord X position (Figure 16) tend to generate blades with swept tips in order to limit compressibility effects for both hover and propeller. The twist distribution is then plot for the three solutions, having clear nonlinear trends especially starting from the 60% of the blade radius.

In particular the P7 solution shows a typical twist distribution for propeller while maintaining anyway excellent hover performance. It is worth noting that as the twist slope increases the propulsive efficiency rises, this is one of the parameter that positively influences propeller mode since the inner portion of the XV15 blade typically acts as a windmill in propeller. Higher twist slope inverts this tendency. As the FoM increases among the optimal solutions (going from P7 to P1) the twist outer than the 60% of the radius becomes highly nonlinear. The local increase in twist (around 80%) is used to counterbalance the local velocity induced by the tip vortex generated by the preceding blade (which generates a reduction of local AoA). This seems to be useful in order to increase the FoM since the blade experiences a more uniform radial distribution of thrust. The nonlinearity is not detrimental in propeller performance for P3. On the contrary the excessive local twist increase, highly decreases the η_P for P1.

The anhedral feature is also shown in Figure 18 which is plotted for the three optimal blades. It is possible to note that for P1 and P3 the maximum possible anhedral (lower bound) is reached meaning that the anhedral is helpful for hover performance. The anhedral has anyway lower influences in propeller conditions.

The performance of the three optimal blades are shown in Figure 19 (hover) and Figure 20 (propeller) using the ADPANEL code (panel method with free-wake). It is possible to note that all the three optimal solutions have the maximum FoM approximately at C_t = 0.012 as requested in the objective and

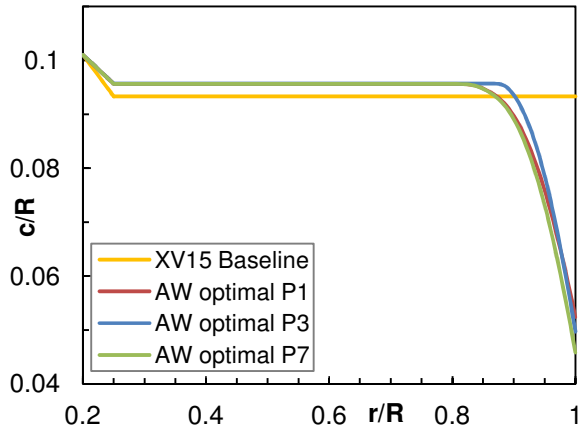

Figure 15: Chord distribution for the optimal blades selected.

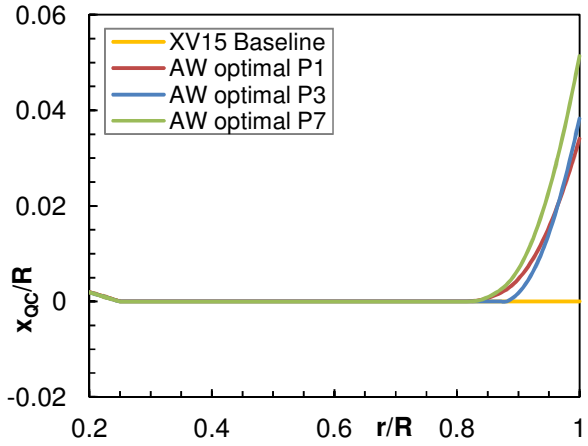

Figure 16: Quarter chord X position distribution for the optimal blades selected.

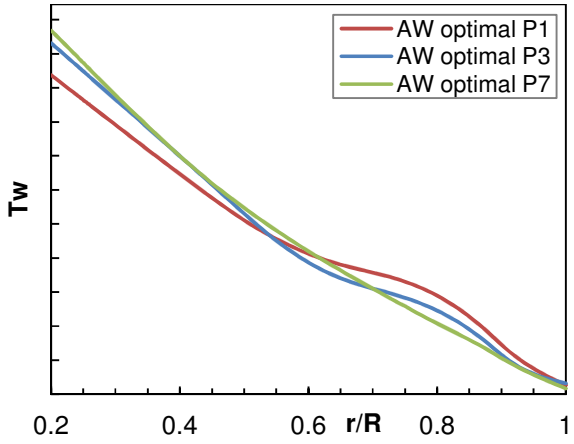

Figure 17: Twist distribution for the optimal blades selected.

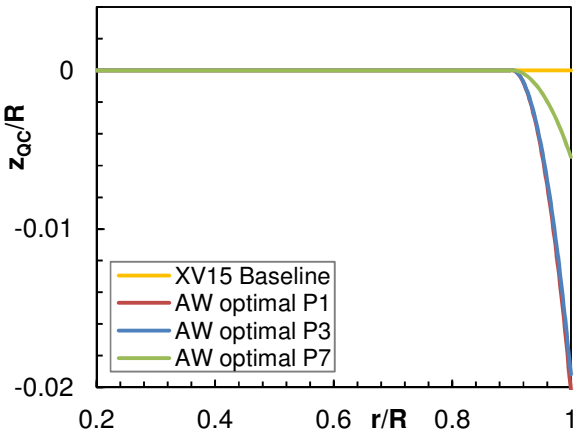

Figure 18: Quarter chord Z position distribution for the optimal blades selected.

contemporary have always higher FoM for the whole C_t range. Similar considerations can be made for the propeller performance increase. It is worth noting that the improvements are widespread all over the thrust range simulated but especially for the optimization range (C_t = 0.002 to 0.006) where the elbow is located.

One of the three optimal solutions, specifically the P3 blade, is selected for further investigations and validations with the Navier-Stokes code HMB. The P3 solution is the best compromise in terms of hover and propeller improvements. The geometry is visible in Figure 21 compared to the XV15 CAD.

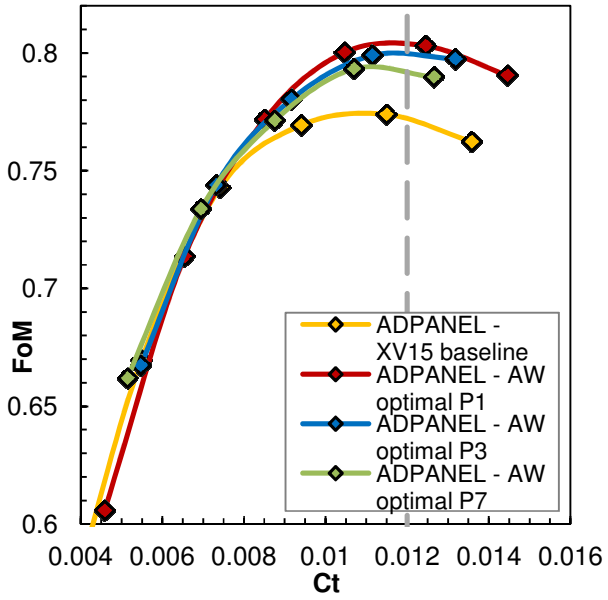

Figure 19: Figure of Merit of the optimal blades selected compared to the XV15 (calculated with ADPANEL). The dashed gray line represent the design objective in hover.

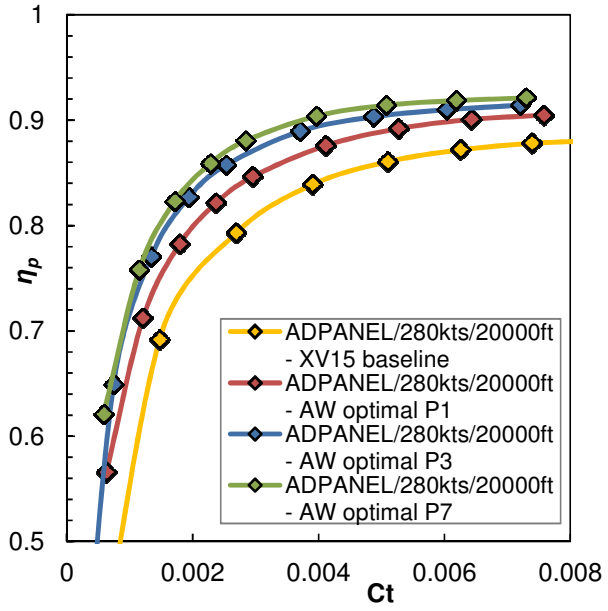

Figure 20: Propeller Efficiency of the optimal blades selected compared to the XV15 (calculated with ADPANEL). The design objective is represented by the improvement of η_P within C_t 0.002-0.006.

Figure 21: Comparison of the baseline XV15 blade geometry and the selected optimal P3.

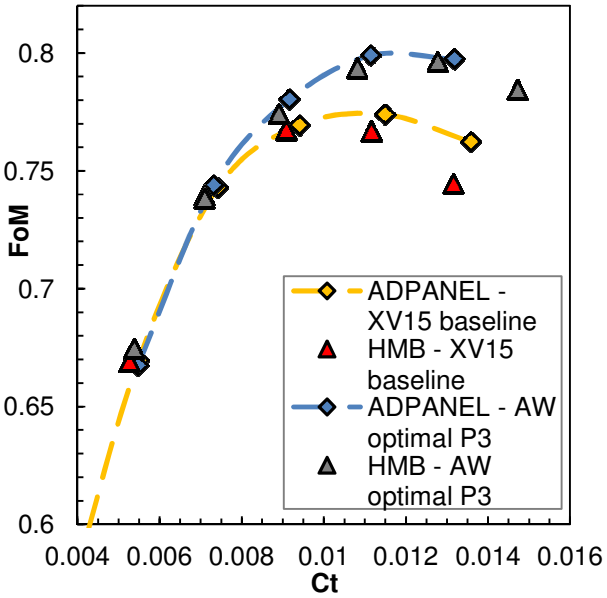

Figure 22: Figure of Merit of the optimal blade P3 compared to the XV15 (validated with HMB).

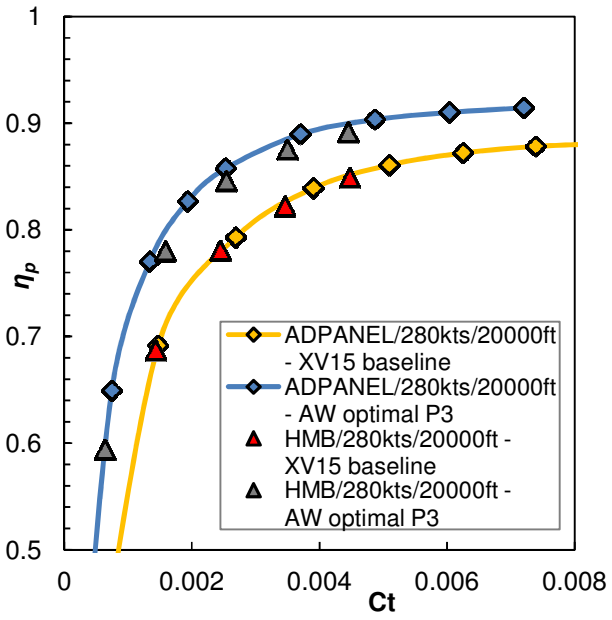

Figure 23: Propeller Efficiency of the optimal blade P3 compared to the XV15 (validated with HMB).

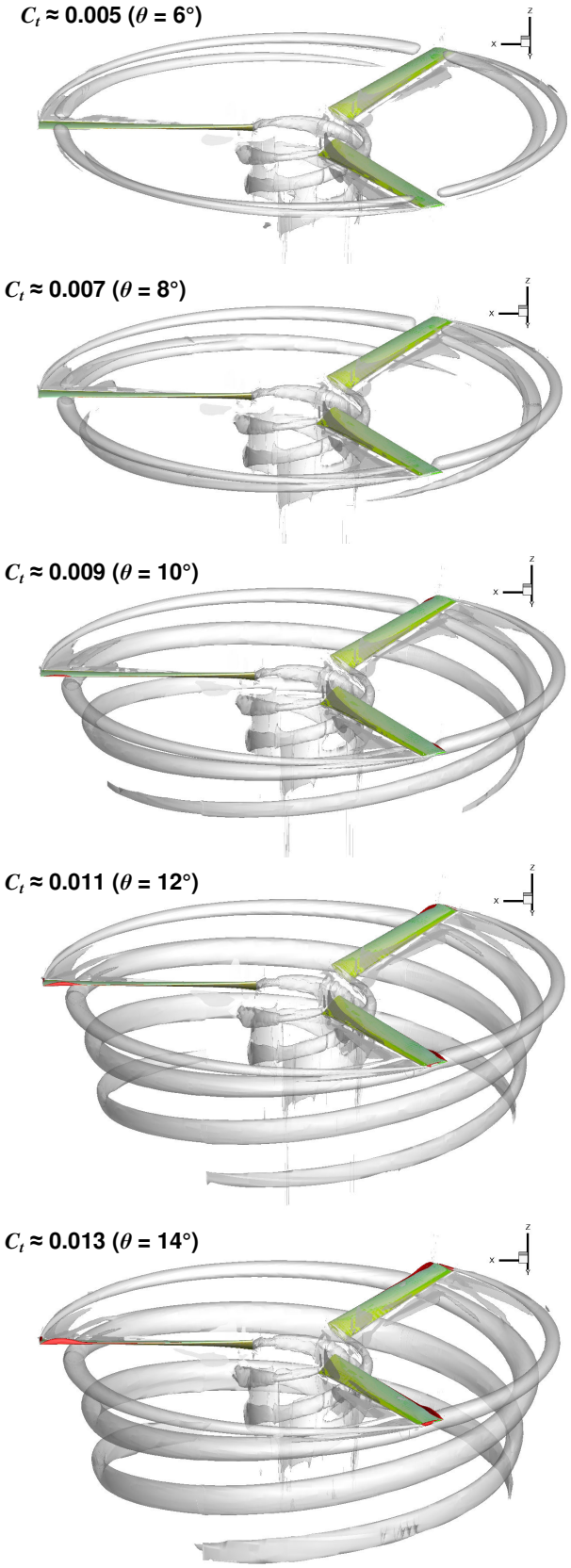

Figure 24: Hover simulations of the baseline XV15 rotor with HMB (wake plot with Q criterion in gray and supercritic zone in red).

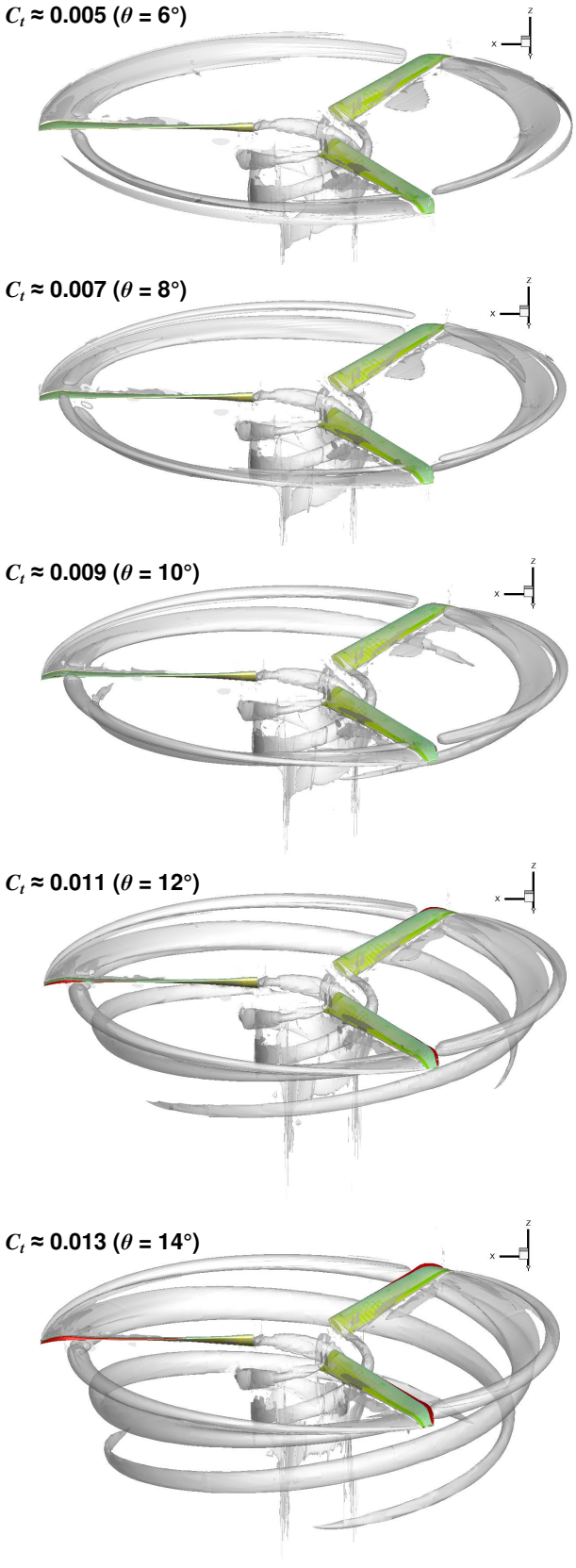

Figure 25: Hover simulations of the optimal P3 rotor with HMB (wake plot with Q criterion in gray and supercritic zone in red).

The outcomes coming from the 3D panel method ADPANEL are verified using the state-of-the-art Navier-Stokes solver HMB both in hover and propeller conditions. The simulations are performed for the P3 optimal blade only and the XV15 baseline. The two rotors' performance as calculated with HMB are compared to the ADPANEL ones and plotted in Figure 22 (hover) and Figure 23 (propeller). It is possible to note only small discrepancies between the two codes at the highest collective values simulated for the XV15 baseline rotor, as already mentioned, but the N-S code confirms the improvements in FoM as obtained with ADPANEL, showing that the new optimal rotor has better performance for all the thrust range simulated and enhanced stall margins. Similar considerations can be stated for the propeller Efficiency. The HMB simulations perfectly follow the panel method solution of the XV15 rotor and similarly for the P3 optimal blade. The panel method slightly overestimates the propeller improvements when compared to the N-S solutions, going from about 6.3% to 5.8% of benefit in efficiency.

The N-S simulations are also reported in a visual layout in Figure 24 and Figure 25 for hover and Figure 26 and Figure 27 for propeller. In the pictures it is possible to observe the wake development by means of the Q criterion and the zones of supercritic flow. In hover the supercritic zones are reduced on the optimal P3 blade and, above all, they are largely smoothed and more uniformly distributed along the blade. The wake development drastically changes

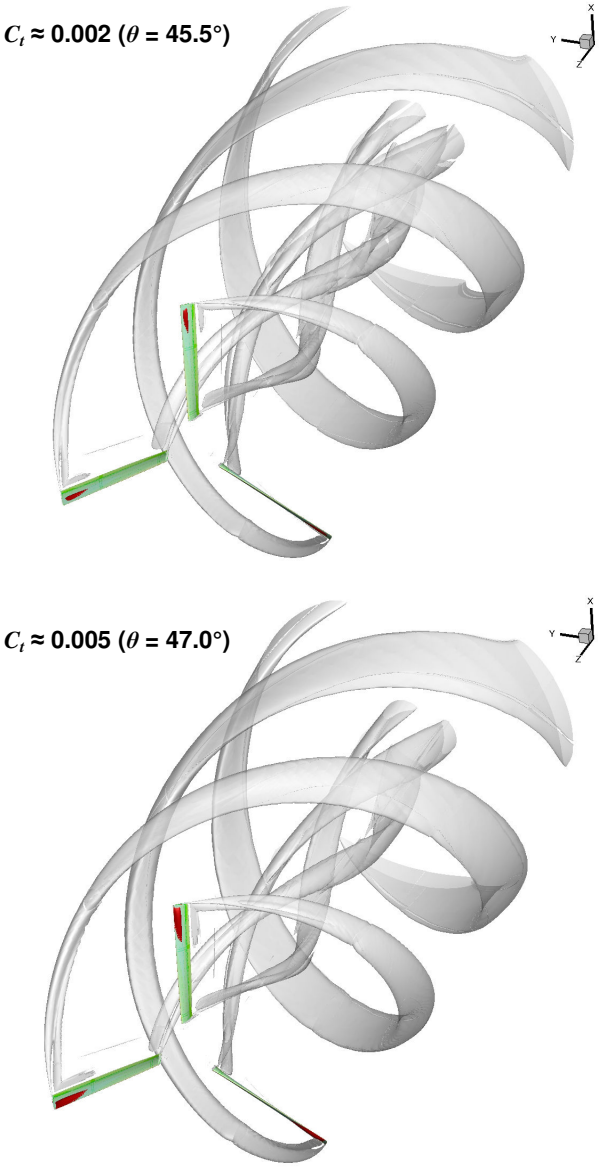

Figure 26: Propeller simulations of the baseline XV15 rotor with HMB (wake plot with Q criterion in gray and supercritic zone in red).

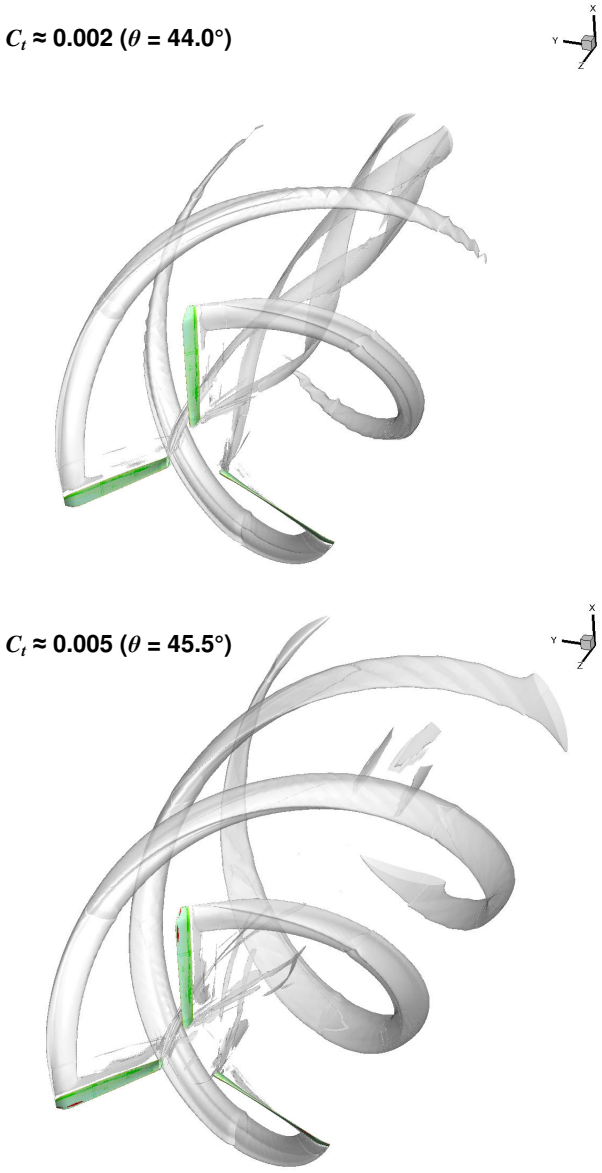

Figure 27: Propeller simulations of the optimal P3 rotor with HMB (wake plot with Q criterion in gray and supercritic zone in red).

going from the XV15 technology to the optimal P3 blade. The swept tip (together with the specific combination of twist and anhedral) generates a sheet of vortices on the last 20% portion of the blade which tends to merge the tip vortex generated by the preceding blade. The tip vortex of the P3 has always lower intensity. Regarding the propeller conditions the two rotors are simulated at 280kts (20000ft altitude) for approximately thrust levels of C_t = 0.002 and C_t = 0.005. Once again the supercritic zone is highly reduced and almost disappears in the simulated conditions. The wake development shows a change in shape and a general reduction of intensity and vortex extension. While on the XV15 rotor simulations the tip vortex appears to be the most relevant vorticity source, on the P3 rotor the vortex sheet released by the swept tip is merged with the tip vortex and modifies the wake development. The simulation results are completed with the hover and propeller loads showing the main differences of thrust and torque distributions between the two blades. In Figure 28 the hover is described showing a more uniform thrust distribution and a smoother tip lift reduction due to the swept planform. The root, thanks to the enhanced performance of the airfoils, demonstrates a higher thrust while the tip is unloaded. The propeller load distributions (Figure 29) are also visible. The XV15 rotor has a clear division between inner part acting as a windmill and the outer part acting as a propeller. This solution anyway leads to a low efficiency middle zone where the thrust reverses. The P3 rotor uses the whole blade as propeller (a part some very low collective pitch conditions) but reducing the tip loads.

6 CONCLUSIONS

An optimization framework for tiltrotor rotor design has been developed, which is based on a state-of-the-art multi-objective surrogate-assisted memetic algorithm coupled with specific aerodynamic simulation tools. The framework is able to optimize 2D airfoils as well as complete rotor blades with the aim of maximizing the global rotor performance of tiltrotors. This optimization methodology has been applied to the redesign of airfoils and rotor of the XV15 aircraft in order to prove its effectiveness. Comparison of final optimal airfoils and rotor blades with the existing XV15 technology yield to the

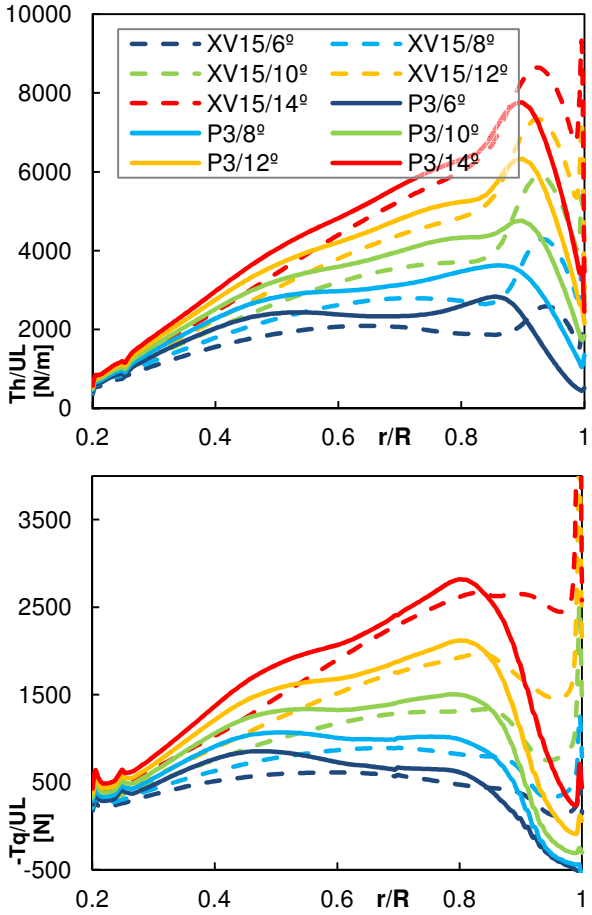

Figure 28: Sectional thrust per unit length (top) and torque per unit length (bottom) in hover for baseline XV15 and optimal P3 rotor.

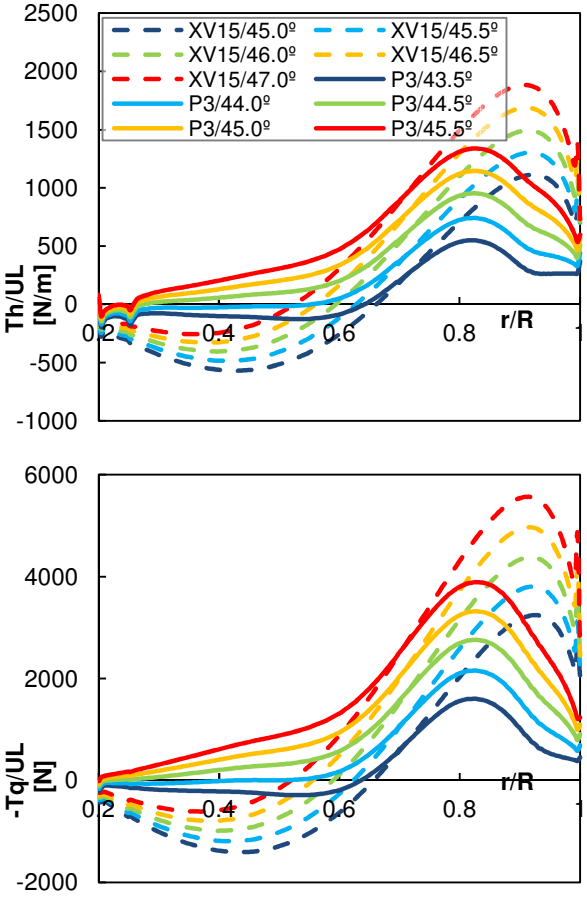

Figure 29: Sectional thrust per unit length (top) and torque per unit length (bottom) in propeller for baseline XV15 and optimal P3 rotor.

following conclusions:

- The framework is capable of optimizing airfoils for tiltrotor's specific conditions. The high demanding operative conditions required to the blade's airfoils when the rotor operation turns from hover to propeller lead to challenging optimization problems which require to take into account many operative points and objectives/constraints for a single airfoil optimization. The intrinsic multi-point and multi-objective nature of the SAMA optimizer can easily handle such problems.

- The optimization of the baseline XV15 airfoil set led to the improvement of specific aerodynamic characteristics of the sections, such as maximum lift, required for maximum thrust capabilities and maneuverability, and drag divergence Mach, helpful for efficient propeller flight. The new optimal airfoils has been tested on the baseline XV15 planform producing slight improvements in hover retarding the FoM drop at high thrust and leaving almost unchanged the propeller performance.

- The optimization of the rotor planform/twist led to excellent improvement of the rotor performance both in hover and propeller. The FoM has been increased from 3 to 4% reaching a maximum value above 0.8 while the propulsive efficiency has been increased up to 8%.

- The 3D panel method with coupled free-wake demonstrated to be an excellent and efficient tool for the optimization framework, since it assures fast simulations (compared to N-S solvers) maintaining very high accuracy in performance prediction. The optimal rotors have been tested and verified with the HMB N-S solver providing practically the same results of the panel method.

- Looking at the rotor optimization it has been confirmed by the results that the twist has the major influence on the rotor performance and advanced nonlinear twist profiles must be investigated in order to obtain the highest possible enhancement of rotor performance for tiltrotors.

7 FUTURE WORKS

Present work and conclusions are related to the development of a complete framework for the aerodynamic optimization of rotor blades for tiltrotors. The application to the XV15 aircraft has been used in order to prove the capabilities of the developed tool and methodology. The optimization framework demonstrated good flexibility and performance, thus it permits further improvements and feature addition. The main future ameliorations to the framework are listed below:

- The tools coupled to the main optimizer can be improved in order to provide a global perfection of the framework. The ADPANEL tool will be completed with an internal trimmer that avoid to the optimizer the need to trim itself each flight condition. In addition the panel method implemented can be easily implemented on a CUDA-based environment taking advantage of the great capabilities of such technology and providing a speed-up up to x100 of the solution time, thus highly reduce the total optimization time.

- Additional specialized tools will be coupled to the optimizer in order to make it able to improve different characteristics of the rotors, such as the acoustic emissions and the structural-dynamic behavior. These additional futures make the optimizer able to perform also multi-physics optimizations for tiltrotors.

8 COPYRIGHT STATEMENT

9 REFERENCES

[1] M.D. Maisel, D.J. Giulianetti, and D.C. Dugan, "*The History of the XV-15 Tilt Rotor Research Aircraft: From Concept to Flight*", NASA SP-2000-4517, 2000.

[2] Massaro, A., Benini, E., "*Multi-Objective Optimization of Helicopter Airfoils Using Surrogate-Assisted Memetic Algorithms*", Journal of Aircraft, Vol. 49, No. 2, pp. 375-383, 2012, doi: 10.2514/1.C001017.

[3] Massaro, A., D'Andrea, A., Benini, E., "*Multiobjective-Multipoint Rotor Blade Optimization in Forward Flight Conditions Using Surrogate-Assisted Memetic Algorithms*", Presented at the 37th European Rotorcraft Forum, Gallarate, Italy, Sep. 13-15, 2011.

[4] Cruz, L., Massaro, A., Melone, S., D'Andrea, A., "*Rotorcraft Multi-Objective Trajectory Optimization for Low Noise Landing Procedures*", Presented at the 38th European Rotorcraft Forum, Amsterdam, Sep. 4-7, 2012.

[5] D'Andrea, A., "*Development of a Multi-Processor Unstructured Panel Code coupled with a CVC Free Wake Model for Advanced*

Analysis of Rotorcraft and Tiltrotors", AHS 64th Annual Forum, Montréal, Canada, 2008.

[6] R. Steijl, G.N Barakos, and K.J. Badcock, "*A Framework for CFD Analysis of Helicopter Rotors in Hover and Forward Flight*", Int. J. Numer. Meth. Fluids, Vol. 51, pp. 819-847, 2006.

[7] Johnson, W., "*Camrad/JA - A Comprehensive Analytical Model of Rotorcraft Aerodynamics and Dynamics - Volume I: Theory Manual*", Johnson Aeronautics, 1988.

[8] Bell Textron, "*Advancement of Proprotor Technology, Task I – Design Study Summary*", Bell Helicopter Company Report 300-099-003, NASA CR-114682, 1969.

[9] Betzina, M.D., "*Rotor Performance of an Isolated Full-Scale XV-15 Tiltrotor in Helicopter Mode*", American Helicopter Society Aerodynamics, Acoustics, and Test and Evaluation Technical Specialists Meeting, San Francisco, CA, Jan. 23-25, 2002.

[10] Felker, F. F., Betzina, M. D., Signor, D. B., *"Performance and Loads Data from a Hover Test of a Full-Scale XV-15 Rotor*", NASA TM 86833, 1985.

[11] Light, J. S., "*Results from an XV-15 Rotor Test in the National Full-Scale Aerodynamics Complex*", American Helicopter Society 53rd Annual Forum, Virginia Beach, Virginia, Apr. 1997.

[12] Bell Helicopter Textron, "*Advancement of Proprotor Technology, Task II – Wind-Tunnel Test Results*", Bell Helicopter Company Report 300-099-004, NASA CR-114363, 1971.